buildings

MDPI

Article

Probabilistic Evaluation Method of Wind Resistance of Membrane Roofs Based on Aerodynamic Stability

Weiju Song [1,2,3,*], Hongbo Liu [1,3] and Heding Yu [2]

[1] School of Civil Engineering, Tianjin University, Tianjin 300350, China; hbliu@tju.edu.cn
[2] Huasheng Construction Group Co., Ltd., Ningbo 315016, China; yheding7@gmail.com
[3] School of Civil Engineering, Hebei University of Engineering, Handan 056038, China
* Correspondence: songweiju@hebeu.edu.cn; Tel.: +86-159-2336-3074

Abstract: The membrane structure or membrane roofing system is lightweight and flexible, with wind being the primary cause of structural and membrane material failure. To evaluate the disaster prevention and mitigation capacity of the membrane roofing system and enhance the wind disaster risk management capabilities, this paper studies the exceedance probability evaluation method for different wind resistance requirements of membrane roofs. Taking Hangzhou in China as an example, the design wind speed risk curve fitted by polynomial is obtained by referring to the PEER performance-based seismic design method and considering the randomness of the wind field. A polynomial fitting method is employed to obtain the design wind speed hazard curve. Considering the nonlinear characteristics of the membrane roof structure, the relationship between the roof's wind resistance requirements (vertical displacement limits) and wind speed spectrum values is approximated using a power function. An annual average exceedance probability expression is derived for different normal deformation demand values of the membrane roofs under wind load. Based on this, a wind resistance probability evaluation method for membrane roofs considering aerodynamic stability is proposed, along with specific steps and related analytical formulas. The results indicate that polynomial fitting provides an effective simplification for deriving the annual average exceedance probability expression for the wind resistance demand of membrane roofs. The performance-based wind resistance probability evaluation method allows for obtaining exceedance probability values for different displacement requirements with minimal structural analysis, which enriches the wind resistance design theory of membrane roofs and further ensures the structural safety of tension membrane roofs under wind load.

Keywords: membrane roofing system; probabilistic evaluation; wind-resistant design; wind speed spectrum hazard curve; aerodynamic stability

Citation: Song, W.; Liu, H.; Yu, H. Probabilistic Evaluation Method of Wind Resistance of Membrane Roofs Based on Aerodynamic Stability. *Buildings* **2024**, *14*, 3725. https://doi.org/10.3390/buildings14123725

Academic Editor: Theodore Stathopoulos

Received: 11 November 2024
Revised: 20 November 2024
Accepted: 21 November 2024
Published: 22 November 2024

1. Introduction

In the field of architecture engineering, membrane structures are aesthetically pleasing, highly translucent, environmentally friendly, and energy-efficient. So they are widely used in large public facilities such as sports stadiums, parking lots, and exhibition halls. Membrane structures or membrane roofing systems are lightweight and flexible. "Lightweight" refers to the low mass of the membrane material, making it susceptible to vibration when subjected to external disturbances, with wind loads typically being the primary controlling load. "Flexible" indicates that the stiffness of the membrane material is low, and the stiffness of the membrane surface is derived from the initial tension, which leads to the large vibration deformation of the membrane structure under wind load. The seismic effects on membrane structures can generally be neglected due to their lightweight, while wind loads typically play a controlling role. Therefore, the study of the dynamic response characteristics of membrane structures cannot ignore the effects of wind load, as wind is a main cause of the damage of structures and membrane materials [1–4]. In recent

decades, there have been many damage examples of membrane structures under wind load. In 2003, the membrane roof of Guangzhou Yihe Villa was torn in a summer typhoon rainstorm. In 2004, the membrane roof of the stadium stands at Wenzhou University was completely destroyed by a typhoon. In 2012, the membrane roof of the Pinghu Gymnasium in Jiaxing, Zhejiang province, was torn up in Typhoon Haikui. On 10 November 2013, the famous landmark building in Sanya, Hainan, China—"The Beauty Crown"—was topped by a strong typhoon. On 18 February 2022, a storm hit the Isle of Wight in the United Kingdom, leading to the tearing of the membrane roof of the O2 Arena in London (formerly known as the Millennium Dome). The structural damage to these buildings resulted in huge economic losses. Numerous post-disaster investigations [5–9] have shown that strong wind can cause serious damage to the roof systems of structures and even lead to the collapse of the main structure. With the frequent occurrence of typhoons, the wind damage loss of membrane structure in coastal areas of China is bound to increase further. Of course, many scholars pay attention to the research of the main structure (including materials), which makes the structure more stable and high-performance in various environments [10,11].

In order to provide the basis and reference for disaster prevention and mitigation capacity evaluation of membrane structures and post-disaster government emergency response work, so as to improve the ability of wind disaster risk prevention and control, it is necessary to carry out in-depth research on their wind resistance performance evaluation. Performance-based structural design methods are derived from research on structural seismic methods in the 1990s [12]. In 1996, Collins, K.R. [13] proposed a performance-based structural design method, defining the "performance objective" as the probability of exceeding a given performance level. The Pacific Earthquake Engineering Research Center (PEER) in the United States evaluated seismic design based on structural performance objectives, expressing structural performance objectives through the annual mean probability of exceeding a limit state. This method includes seismic hazard analysis, structural hazard analysis, and structural loss analysis, incorporating four corresponding parameters: intensity measure (IM) of ground motion, engineering demand parameter (EDP), damage measure (DM), and decision variable (DV) [14]. In 2003, F. Jalayer [15] applied the total probability theory and regression analysis method to derive the simplified calculation formula of the average annual exceedance probability corresponding to each limit state by simplifying the model.

Besides earthquake action, the wind load endured by structures also exhibits stochastic characteristics. For super high-rise buildings, flexible long-span roofs, and membrane structures, where the structural stiffness is relatively low and exhibits significant flexibility, wind load becomes the controlling load. Under wind loads, the response of the structure needs to be controlled within a certain range to meet the different functional requirements, such as vibration acceleration control to meet the comfort requirements or vibration displacement control to meet the structural safety. The wind field consists of mean wind and fluctuating wind, with the fluctuating component having obvious stochastic characteristics. Therefore, the study of wind-induced dynamic responses of membrane structures mainly used stochastic vibration and dynamic reliability theory [16]. In 2006, Zhang Linlin et al. [17] used numerical simulation techniques combined with the probability density evolution method to obtain the probability density function of structural fluctuating wind vibration displacement response and conducted wind resistance reliability analysis. In 2013, Liu Xiaoting proposed a fuzzy reliability design method applicable to different comfort requirements for high-rise structures [18]. In 2017, Feng Yuan improved the evaluation standard of wind resistance comfort of high-rise buildings through numerical simulation, wind tunnel tests, and field measurements and conducted wind resistance reliability analysis for such structures [19]. In 2018, Yang Chun et al. took a wind-sensitive high-rise structure as the research object to assess the reliability of wind-induced comfort based on the peak acceleration response of the structure's top under wind loads of different recurrence periods [20]. In 2024, Tan Chunyuan et al. analyzed the

stochastic dynamic response of the transmission tower-line system considering aeroelastic effects using the probability density evolution theory. Finally, they applied the concept of equivalent extreme value to establish the failure criterion of the transmission tower-line system under wind load and performed a refined wind resistance reliability analysis [21].

Comparatively, the theory of performance-based structural wind-resistant design is still in the initial development stage. In 2004, Paulotto et al. proposed the concept of performance-based wind engineering [22]. In 2006, Augusti et al. proposed the performance-based wind-resistant design method (PBWE) by referring to PEER performance-based seismic design method and used this method to design the wind resistance of a pedestrian bridge [23,24]. In 2008, Petrini et al. applied the PBWE method to the wind-resistant design of hangers in suspension bridges [25]. In 2009, John et al. conducted performance-based wind-resistant design for wood frame structures [26]. Petrini et al. established a probabilistic analysis framework for performance-based wind-resistant design [27]. Zhou Yun et al. established the theoretical framework of performance-based wind resistance design according to the characteristics of wind pressure distribution in mainland China and obtained the multi-level design wind pressure value and multi-level wind resistance performance level target suitable for China;[28]. In 2013, He Minjuan et al. applied the PBWE method to performance-based wind-resistant design for tall structures [29]. In 2014, Huang Guoqing et al. proposed a probabilistic evaluation method for wind damage to roof coverings based on wind tunnel test data [30]. In 2016, studies were conducted on the damage evaluation of wind-induced roof coverings both with and without consideration of wind speed variability [31]. Subsequent studies in 2018 examined the wind-induced vulnerability of roofs considering wind load correlation based on Copula functions [32]. In 2022, Li Zhengliang et al. carried out a vulnerability analysis of standing seam roof systems based on multiple performance levels, effectively predicting damage states, failure probability, and wind resistance capacity of these systems [33]. In 2023, Zhang Hao et al. researched the impact of door and window system failures on roof failures in low-rise cold-formed thin-walled steel structures under wind loads [34]. In 2024, Wu Fengbo et al. proposed a comprehensive wind-induced vulnerability analysis method of light steel structures to systematically consider wind-induced losses of both the main structure and the envelope system [35].

Based on the performance-based seismic design method, a probabilistic assessment method for wind-resistant design of membrane roofs considering aerodynamic stability is established in this paper. The rational design parameters obtained from the study of the membrane roof model are used to take the values of geometric parameters and pre-tensions to prevent the occurrence of aeroelastic instability. The stochastic characteristics of wind speed at a specific site are considered, with the mean wind speed assumed to follow the Gumbel distribution and the fluctuating wind speed modeled as a zero-mean stationary Gaussian random process. The derivation method for the closed-form expression of the mean annual exceedance probability for structural seismic limit states by F. Jalayer is referenced, and appropriate assumptions are made to obtain the calculation expression for the mean annual exceedance probability of wind resistance for membrane roofs. Based on this, a probabilistic wind resistance evaluation method for membrane roofs considering aerodynamic stability is proposed, and specific steps and relevant analytical formulas for this evaluation method are provided so as to further ensure the structural safety of membrane roofs under wind load.

2. Wind Hazard Analysis

2.1. Uncertainty Factors

In the study of probabilistic wind-resistant design, it is essential to identify the uncertainty factors present in structural wind engineering. Petrini categorized the uncertainties in structural wind engineering into two types: wind uncertainties and exchange region uncertainties [27,36]. Wind uncertainties, denoted by parameter α, are independent

of the structure and pertain to the randomness in the wind field, including the stochastic nature of mean wind, fluctuating wind, and site-specific uncertainties. Exchange region uncertainties, represented by the independent parameter γ, involve the randomness in the physical parameters of the structure affected by non-wind-related environmental factors. Additionally, the uncertainties arising from the interaction between the wind field and the structure are represented by the derived parameter β. Consequently, the function of uncertainty parameters in structural wind engineering can be expressed as $\Theta(\alpha, \beta, \gamma)$. To simplify the derivation process, this study focuses solely on the influence of stochastic wind field parameters, excluding random structures, so the conditional probability relationship among the three parameters is as follows:

$$P(\alpha|\beta) = P(\alpha)$$
$$P(\alpha, \beta, \gamma) = P(\beta|\alpha) \cdot P(\alpha)$$

2.2. The Probabilistic Model of Wind Fields

For wind-resistant design, it is essential that the design extreme wind speeds for different recurrence periods at the site are reasonably provided, as this forms the basis and prerequisite for accurate design [37]. Since extreme wind speeds involve probabilistic calculations, their statistical probability density function and distribution function must be obtained. For the probabilistic modeling of annual extreme wind speeds, three types of distributions are typically considered: the Gumbel distribution, the Frechet distribution, and the Weibull distribution. Initially, annual extreme wind speeds were believed to follow the Frechet distribution. However, increasing research has demonstrated that annual extreme wind speeds align more closely with the Gumbel distribution. Currently, the calculation of design wind speeds generally involves fitting annual maximum wind speeds with the Gumbel distribution, after which a design wind speed suitable for engineering use is provided under a certain reliability level [38].

The "Unified Standard for Reliability Design of Building Structures" (GB15112-10384) [39] in China adopts this method for analyzing the wind load of the site. In this approach, long-term statistical samples of local wind speeds are required, with at least 30 years of wind speed observation records typically considered necessary. It is also assumed that the annual maximum wind speeds are independent, stationary, and conform to the Gumbel distribution [39]. Therefore, the annual mean maximum wind speed at the site is fitted using the Gumbel distribution in this paper, with its probability distribution function expressed as,

$$F(x) = \exp(-\exp(-(x-\beta)/\alpha)) \tag{1}$$

where α and β are scale parameters and position parameters, respectively, and the relationship with the mean μ and variance σ^2 of the Gumbel distribution is calculated as follows:

$$\mu = \beta + \nu\alpha$$
$$\sigma^2 = \frac{\pi^2\alpha^2}{6} \tag{2}$$

where, $\nu = 0.57722$ is the Euler constant.

Then,

$$\mu = \overline{X}$$
$$\sigma^2 = S_x^2 \tag{3}$$

The estimated values $\hat{\alpha}$ and $\hat{\beta}$ of parameters α and β can be obtained from Equations (2) and (3) as follows:

$$\begin{aligned} \hat{\alpha} &= \frac{2.4495}{\pi} \cdot S_x \\ \hat{\beta} &= \bar{X} - 0.45005 \cdot S_x \end{aligned} \tag{4}$$

Currently, the annual maximum wind speed V_{10} at a height of 10 m is used as the statistical sample for wind speed across various regions in China [40]. The probability distribution function is written as follows:

$$F(V_{10}) = \exp(-\exp(-(V_{10} - \beta)/\alpha)) \tag{5}$$

Substituting Equation (4) into Equation (5), yields the following:

$$F(V_{10}) = \exp(-\exp(\frac{-(V_{10} - \bar{X} + 0.45005 \cdot S_x)}{\frac{2.4495}{\pi} \cdot S_x})) \tag{6}$$

The design maximum wind speed V_m for a design return period T_0 is as follows:

$$V_m = \bar{X} - \frac{2.4495}{\pi} S_x \cdot \left[0.5772 + \ln\left(-\ln P_0\right)\right] \tag{7}$$

where $P_0 = 1 - \lambda = 1 - \frac{1}{T_0}$ and λ represent the mean annual exceedance probability, and $\lambda = \frac{1}{T_0}$.

The mean annual exceedance probability corresponding to the design maximum wind speed V_m is as follows:

$$\lambda\left(V_m\right) = 1 - \exp\left(-\exp\left(\frac{-(V_m - \bar{X} + 0.45005 \cdot S_x)}{\frac{2.4495}{\pi} \cdot S_x}\right)\right) \tag{8}$$

For engineering structures, wind speed is generally represented by wind pressure. The "Load Code for the Design of Building Structures" GB50009-2012 [40] lists wind pressure values w for different regions in China, corresponding to return periods of 10, 50, and 100 years. Then, the design maximum wind speed V_m can be derived. For instance, in Hangzhou, the basic wind pressure for a 10-year return period is 0.25 kN/m^2, for a 50-year return period is 0.40 kN/m^2, and for a 100-year return period is 0.45 kN/m^2. Using Bernoulli's equation yields the following:

$$w_a V + \frac{1}{2} m v^2 = C \tag{9}$$

where $w_a V$ is the static pressure energy. Dividing both sides of Equation (9) by V yields the following:

$$w_a + \frac{1}{2} \rho v^2 = C_1$$

The wind pressure per unit area provided by the wind speed of a free airflow can be expressed as follows:

$$w = \frac{1}{2}\rho v^2 = \frac{1}{2}\frac{\gamma}{g}v^2$$

where

w is the wind pressure;
ρ is the air density;
v is the wind speed.

The above equation is the commonly used relationship between wind speed and wind pressure. In Chinese regulations, the coefficient is taken as 1/1600. Thus, we obtain the following:

$$V = \sqrt{1600w} \tag{10}$$

From Equation (10), the maximum design wind speeds for Hangzhou, China, with return periods of 10 years, 50 years, and 100 years can be calculated as $V_m(10) = 20.00\text{m/s}$, $V_m(50) = 25.30\text{m/s}$, and $V_m(100) = 26.83\text{m/s}$, respectively. By substituting these wind speed values into Equation (5), the mean value $\overline{X}$=14.591m/s and standard deviation S_x=4.115m/s of V_{10} for Hangzhou can be determined. These calculated mean and standard deviation values can then be substituted into Equation (6) to obtain the mean annual exceedance probability curve for the corresponding design maximum wind speed, which is the maximum design wind speed hazard curve:

$$\lambda\left(V_m\right) = 1 - \exp\left(-\exp\left(\frac{-(V_m - 12.74)}{3.21}\right)\right) \tag{11}$$

Applying the least squares method, the curve drawn from Equation (11) is approximated using a fifth-degree polynomial. The resulting fitting function, as shown in Figure 1, is calculated as follows:

$$\lambda\left(x\right) = c_0 + c_1 x + c_2 x^2 + c_3 x^3 + c_4 x^4 + c_5 x^5 \tag{12}$$

where

$c_0 = 1.52,\ c_1 = -0.4042,\ c_2 = 0.0486,\ c_3 = -0.003117,\ c_4 = 0.0001027,$
$c_5 = -1.357 \times 10^{-6}$

The fitting model is analyzed by variance, and the sum of squares R^2 is used to evaluate the fitting effect of the fitting function. R^2 value closer to 1 indicates a better fit [41]. The analysis yielded an R^2 value of 0.99617 for the fifth-order polynomial fitting, which is very close to 1, demonstrating an excellent fitting performance.

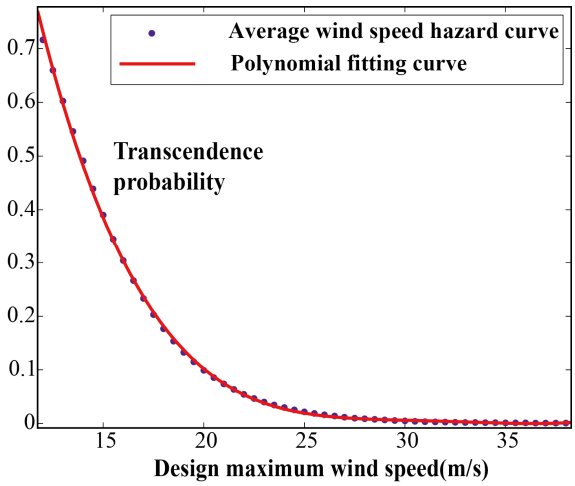

Figure 1. Annual average wind speed hazard curve.

2.3. Stochastic Characteristics of Wind Speed

Based on extensive wind speed measurement records and time series analysis, it has been found that, if the severe non-stationary segments near the initial stage are discarded, the wind can be approximated as a nearly stationary random process. Therefore, fluctuating wind is often considered a zero-mean Gaussian stationary random process with ergodic properties. Its statistical characteristics can be described by several methods, such as the power spectral density function. In structural wind resistance, the Davenport spectrum is commonly used to represent the self-power spectrum of longitudinal horizontal fluctuating wind speed [42]. According to more than 90 strong wind records measured at different places and heights around the world, and assuming that the turbulence integral scale L is a constant value of 1200 m, Davenport established the empirical formula of the pulsating wind speed spectrum as follows [43]:

$$S_v(\omega) = \frac{4Kf^2}{\omega(1+f^2)^{4/3}}\bar{V}_{10}^2 \tag{13}$$

where $f = \frac{1200\omega}{\bar{V}_{10}}$ and ω are the frequency of the fluctuating wind; K is the surface roughness coefficient that varies with different terrain conditions. Davenport, based on field measurements, summarized the K values for various sites, as shown in Table 1 [44].

Table 1. Summary of measured site K values of Davenport.

Surface Type	River Bay	Open Land	Low Trees at 10 m Height	Town	Bustling City
K	0.003	0.005	0.015	0.030	0.050

Unfortunately, the values provided in Table 1 have limited practicality. The paper "Calculation Formula for the Coefficient K in the Davenport Spectrum and Its Engineering Application" derived the calculation formula for the wind speed spectrum based on random vibration theory and China's load code. It established a relationship between the surface roughness coefficient and the ground roughness index α, as follows:

$$K = \frac{1}{6\times 8.8^2}\times 3.5^{3.6(\alpha-0.16)} \tag{14}$$

According to the "Code for Design of Building Structures Load" (GB50009-2012), the *K* values corresponding to the four types of terrain in China are shown in Table 2.

Table 2. *K* values of four geomorphologic types in China.

Geomorphologic Types	A	B	C	D
α	0.12	0.15	0.22	0.30
K	0.00129	0.00206	0.0046	0.0129

Since the crosswind and vertical fluctuating wind speed spectra are much smaller than the longitudinal wind speed spectrum [45], the influence of vertical and crosswind fluctuating wind speeds is not considered in this study in order to simplify the calculations.

Commonly used methods to simulate the time history of fluctuating wind speed include the AR method and the WAWS method [46]. Both methods can simulate multiple related wind speed time histories. The AR method is widely used due to its advantages, such as high computational efficiency [47,48]. Therefore, this paper adopts the AR method for wind speed time series simulation. The AR model converts a random white noise series with a mean of 0 into a stationary random process with specified spectral characteristics through linear filtering.

The system gain is defined as *G*, and the system function H(z) is calculated as follows:

$$H(z) = \frac{G}{1 + \sum_{i=1}^{p} a_i z^{-i}} \tag{15}$$

Assuming that the output $x(n)$ is excited by white noise $w(n)$, the time-domain expression of the model can be written as follows:

$$x(n) + \sum_{i=1}^{p} a_i x(n-i) = Gw(n) \tag{16}$$

The recursive relationship for the AR (Autoregressive) model is as follows:

$$R_x(m) = \begin{cases} -\sum_{i=1}^{p} a_i R_x(m-i), m = 1, 2, \cdots, p \\ -\sum_{i=1}^{p} a_i R_x(i) + G^2, m = 0 \end{cases} \tag{17}$$

Under the premise of meeting engineering accuracy requirements, the following assumptions are made for the wind speed time series [43,49]:

The mean wind speed at any point is independent of time.

The fluctuating wind speed time series is a zero-mean stationary random process.

The wind speed time series exhibits spatial correlation.

These assumptions simplify the analysis and simulation of wind speed data, making it more manageable while still capturing the essential features of the wind environment relevant to engineering design.

The AR model for the spatially correlated fluctuating wind speed time series at multiple points, represented as a column vector $V(x, y, z, t)$ is as follows [50]:

$$V(x, y, z, t) = \sum_{k=1}^{p} \psi_k V(x, y, z, t - kVt) + N(t) \tag{18}$$

where $x = [x_1, x_2, L, x_M]^T$, $y = [y_1, y_2, L, y_M]^T$, $z = [z_1, z_2, L, z_M]^T$, and (x_i, y_i, z_i) are the spatial coordinates of the *i*-th point, p, is the order of the AR model; Δt is the time step

for simulating the wind speed time series; and ψ_K is the autoregressive coefficient matrix at lag k, where $k = 1, 2, \ldots, p$, $N(t)$ is the vector of independent random processes at time t, representing the white noise input.

$$N(t) = L \cdot n(t) \tag{19}$$

where $n(t) = \left[n_1(t), \cdots n_M(t)\right]^T$, $n_i(t)$ represents a random process with a mean of 0 and variance of 1.

$$R \cdot \psi = \begin{bmatrix} R_N \\ O_P \end{bmatrix} \tag{20}$$

$$\psi = \left[I, \psi_1, \cdots \psi_P\right]^T \tag{21}$$

$$R_N = R_0 + \sum_{k=1}^{p} \psi_k R\left(kVt\right) \tag{22}$$

where ψ is a $(p+1)\mathrm{M} \times \mathrm{M}$-dimensional matrix and I is an M-dimensional identity matrix, where all diagonal elements are 1 and off-diagonal elements are 0; O_p is a pM×M-dimensional matrix, with all elements equal to 0; and R is a $(p+1)$M × $(p+1)$M-dimensional autocorrelation matrix, specifically a Toeplitz matrix. The matrix R can be expressed as follows:

$$R = \begin{bmatrix} R_{11}(0) & R_{12}(Vt) & R_{13}(2Vt) & \cdots & R_{1(p+1)}(pVt) \\ R_{21}(Vt) & R_{22}(0) & R_{23}(Vt) & \cdots & R_{2(p+1)}[(p-1)Vt] \\ R_{31}(2Vt) & R_{32}(Vt) & R_{33}(0) & \cdots & R_{3(p+1)}[(p-2)Vt] \\ \vdots & \vdots & \vdots & \ddots & \vdots \\ R_{(p+1)1}(pVt) & R_{(p+1)2}[(p-1)Vt] & R_{(p+1)3}[(p-2)Vt] & \cdots & R_{(p+1)(p+1)}(0) \end{bmatrix}_{(p+1)M \times (p+1)M}$$

Where $R_{ij}(mVt)$ is a M×M-dimensional matrix.

The relationship between the power spectral density (PSD) and the autocorrelation function is as follows:

$$R_{ij}(\tau) = \int_0^\infty S_{ij}(f) \cos\left(2\pi f \cdot \tau\right) df, i, k = 1, \cdots, M \tag{23}$$

where f is the frequency of the fluctuating wind speed. When $i = j$, $S_{ij}(f)$ represents the autocorrelation spectral density function of the fluctuating wind speed; when $i \neq j$, $S_{ij}(f)$ represents the cross-spectral density function of the fluctuating wind speed, which can be determined from the autocorrelation spectral density function $S_{ii}(f)$ and the coherence function $r_{ij}(f)$.

$$S_{ij}(\tau) = \sqrt{S_{ii}(f) S_{jj}(f)} \cdot r_{ij}(f) \tag{24}$$

$$r_{ij}(f) = \exp\left[\frac{-2n\sqrt{C_x^2(x-x')^2 + C_y^2(y-y')^2 + C_z^2(z-z')^2}}{\overline{v}(z) + \overline{v}(z')}\right] \tag{25}$$

$$\overline{v}(z) = \overline{v}(10)\left(\frac{z}{10}\right)^{\alpha} \tag{26}$$

where $\overline{v}(10)$ can be calculated based on the local basic wind pressure values provided in the "Building Structural Load Code" (GB50009-2012). The procedure is as follows:

$$\overline{v}_{10} = \sqrt{2g\omega_{10}/\rho} \tag{27}$$

Davenport spectrum is adopted for power spectra $S_{ij}(f)$ and $S_{ii}(f)$ in Equation (27), C_x, C_y, and C_z are attenuation coefficients, and Borri. C. suggests C_x = 6, C_y = 16, C_z = 10.

By solving the linear equations given in (22), the regression coefficient matrix ψ can be obtained.

Performing Cholesky decomposition on the matrix R_N, determined from Equation (23), yields the following:

$$R_N = L \cdot L^T \tag{28}$$

It can be obtained from Equation (18), as follows:

$$\begin{bmatrix} v^1(j \sim t) \\ \vdots \\ v^M(j \sim t) \end{bmatrix} = -\sum_{k=1}^{p} \psi_k \cdot \begin{bmatrix} v^1[(j-k) \sim t] \\ \vdots \\ v^M](j-k) \sim t] \end{bmatrix} + \begin{bmatrix} N^1(j \sim t) \\ \vdots \\ N^M(j \sim t) \end{bmatrix}, \begin{pmatrix} j \sim t = 0, \cdots, T \\ k \le j \end{pmatrix} \tag{29}$$

In the calculation, it is assumed that the wind speed before the initial moment is 0, i.e., $V = 0$ at $t \le 0$. The final wind speed time series is given by the following:

$$V(t) = \overline{v}(z) + v(t) \tag{30}$$

The fluctuating wind characterized by the wind speed power spectral density function in the frequency domain is transformed into the wind speed time series in the time domain. Taking a flat membrane roof model as an example, the total wind speed time series at various wind speed simulation points on the roof is calculated when the roof is fully enclosed with a wind direction angle of 0°.

The dimensions of the roof are 20 m × 20 m. The roof is divided into 12 regions, and the wind speed time series is simulated at the central location of each region. The corresponding point numbers of the simulation locations are shown in Figure 2. The basic wind pressure is 0.25 kN/m², and the ground roughness category is Class D. The cutoff frequency is 20 Hz, and the initial frequency is 0.001 Hz. The sampling time interval Δt is required to be no smaller than 0.1 s, so Δt = 0.1 s is chosen. The autoregressive order is determined to be p = 4, and the number of time steps is N = 1024. The wind pressure distribution coefficients used in the wind load simulation are referenced from the wind pressure distribution coefficients for flat roofs in [51], as shown in Figure 2.

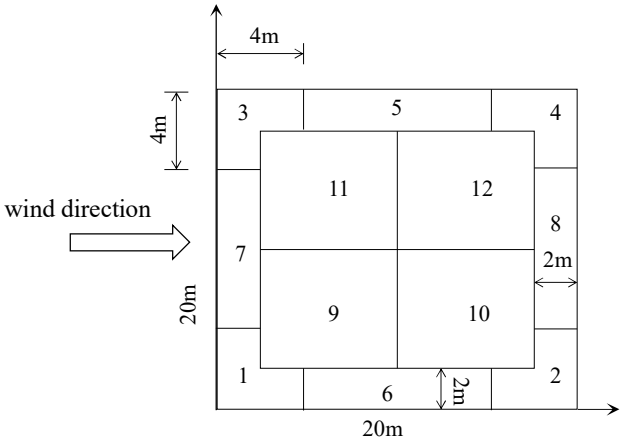

Figure 2. Position diagram of wind speed simulation point.

Taking point 7 in Figure 2 as an example, considering the temporal and spatial correlation, the wind speed time history curve is randomly generated by MATLAB R2021b [52], as shown in Figure 3a. By comparing the power spectral density curve of the simulated wind speed at the node with the target power spectral density curve, as shown in Figure 3b, it can be demonstrated that the power spectral density of the wind speed obtained from the simulation matches well with the target power spectral density across a wide range of frequencies. This indicates that the simulation method used in this paper can effectively capture the statistical characteristics of wind speed fluctuations.

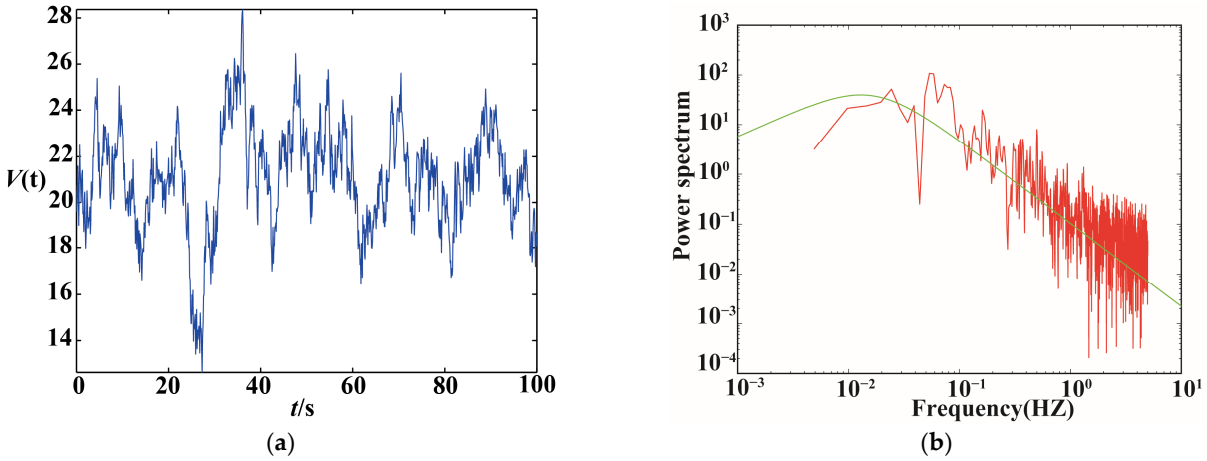

Figure 3. Simulated wind speed time history curve and simulated wind speed power spectral density curve. (**a**) Simulated wind speed time history curve at point 7; (**b**) Simulated wind speed power spectral density curve at point 7.

3. Response Time History Analysis Considering Additional Air Quality of Membrane Roofing

The wind-induced vibration response of the membrane roof is solved using a nonlinear time-domain analysis method. The Newmark–β method is the most commonly used in the nonlinear dynamic calculation of the membrane roof system, and it is the method selected in this study.

The nonlinear dynamic differential equation of the membrane structure under the action of fluctuating wind is as follows:

$$[M]\{\ddot{U}\}+[C]\{\dot{U}\}+[K]\{U\}=\{P\} \quad (31)$$

where the mass matrix $[M]$ is the lumped mass matrix, the damping matrix $[C]$ adopts Rayleigh damping, $[K]$ is the stiffness matrix, and $\{P\}$ is the wind load vector on each node of the structure.

The wind load acting on the position of node i can be expressed as follows:

$$P_i(t) = P_{i1}(t) + P_{i2}(t) \tag{32}$$

Considering the effects of average wind and pulsating wind, the wind load is as follows:

$$P_{i1}(t) = \frac{1}{2} C_p \rho A (\overline{V} + v(t))^2 \tag{33}$$

where C_p is the wind pressure distribution coefficient for the membrane roof, which is determined based on the pressure distribution coefficient for flat roofs as referenced in [51]; ρ is the air density, with a value of $\rho = 1.226 \text{kg/m}^3$; A is the area corresponding to the node; $\overline{V}$ is the average wind speed; and $v(t)$ is the fluctuating wind speed.

In Equation (32), the inertial load generated by the additional air quality on the inner side of the membrane roof can be expressed as follows:

$$P_{i2}(t) = -m_a \frac{\partial^2 U}{\partial t^2} \tag{34}$$

In Equation (34), ma is the additional air mass. For a flat membrane roof, the analytical expression for the additional air mass is as follows [53]:

$$m_a = \frac{-\int_0^b \int_0^a p \frac{\partial w(x,y,t)}{\partial t} dxdy}{\int_0^b \int_0^a \frac{\partial w(x,y,t)}{\partial t} \cdot \frac{\partial w^2(x,y,t)}{\partial t^2} dxdy} \tag{35}$$

where ma represents the additional mass per unit area, P is the aerodynamic pressure on the membrane during the vibration process, and $w(x, y, t)$ is the displacement function of the roof during the vibration process.

In calculating the additional air mass ma, for convenience, the first-order vibration mode is considered. The wind speed is taken as the design wind speed for the recurrence period, and the specific membrane material parameters are substituted to solve for the additional air mass. Taking the basic wind pressure of 0.25 kN/m² for the 10-year recurrence period in the Hangzhou area as an example, it is converted into a design maximum wind speed of 20 m/s, with an initial pre-tension of 3 kN and a membrane size of $a = b =$ 20 m. Using the ma calculation formula and process, the result is $m_a = 1.27$ ms, where ms is the material density. Therefore, Equation (34) can be written as follows:

$$P_{i2}(t) = -1.27 \frac{\partial^2 U}{\partial t^2} \tag{36}$$

When calculating the stiffness matrix, the additional air mass is converted into the membrane material density. This is equivalent to an increase in the membrane material density due to the presence of the additional mass. In the example above, due to the additional mass, the membrane material density changes from m_s to 2.27× m_s.

The dynamic equilibrium equation of the structure at time t can be expressed as follows:

$$[M]\{\ddot{u}\}_t + [C]\{\dot{u}\}\{\ddot{u}\}_t + [K]\{u\}\{\ddot{u}\}_t = \{P(u(t), t)\}$$

The dynamic equilibrium equation of the structure at time $t+\Delta t$ can be expressed as follows:

$$[M]\{\ddot{u}\}_{t+\Delta t}+[C]\{\dot{u}\}_{t+\Delta t}+[K]\{u\}_{t+\Delta t}=\{P(u(t+\Delta t),t+\Delta t)\}$$

The velocity and displacement of the structure at time $t+\Delta t$ can be expressed in the following expanded form:

$$\{\dot{u}\}_{t+\Delta t}=\{\dot{u}\}_t+[(1-\gamma)\{\ddot{u}\}_t+\gamma\{\ddot{u}\}_{t+\Delta t}]\cdot\Delta t$$

$$\{u\}_{t+\Delta t}=\{u\}_t+\{\dot{u}\}_t\cdot\Delta t+[(\frac{1}{2}-\beta)\{\ddot{u}\}_t+\beta\{\ddot{u}\}_{t+\Delta t}]\cdot\Delta t^2$$

By introducing the initial condition $\{u\}_0$, $\{\dot{u}\}_0$, $\{\ddot{u}\}_0$, the displacement value at time $t+\Delta t$ can be obtained from the following equilibrium relation:

$$\left[\tilde{K}\right]_{t+\Delta t}\{u\}_{t+\Delta t}=\left\{\tilde{F}\right\}_{t+\Delta t}$$

$$\left[\tilde{K}\right]_{t+\Delta t}=[K]_{t+\Delta t}+[M]\frac{1}{\beta\cdot\Delta t^2}+[C]\frac{\gamma}{\beta\cdot\Delta t}$$

$$\left[\tilde{F}\right]_{t+\Delta t}=\{F(u_{t+\Delta t},t+\Delta t)\}+[M][\{u\}_t\frac{1}{\beta\cdot\Delta t^2}+\{\ddot{u}\}_t\left(\frac{1}{2\beta}-1\right)]$$

$$+[C][\{u\}_t\frac{\gamma}{\beta\cdot\Delta t}+\{\dot{u}\}_t\left(\frac{\gamma}{\beta}-1\right)+\{\ddot{u}\}_t\cdot\frac{\Delta t}{2}\left(\frac{\gamma}{\beta}-2\right)]$$

The velocity and acceleration at time A and B can be obtained from above equations.

Therefore, the velocity and acceleration at moments *t* and $t+\Delta t$ are written as follows:

$$\{\ddot{u}\}_{t+\Delta t}=\frac{1}{\beta\cdot\Delta t^2}\{\{u\}_{t+\Delta t}-\{u\}_t\}-\frac{1}{\beta\cdot\Delta t}\{\dot{u}\}-\left(\frac{1}{2\beta}-1\right)\{\ddot{u}\}_t$$

$$\{\dot{u}\}_{t+\Delta t}=\{u\}_t+\Delta t(1-\gamma)\cdot\{\dot{u}\}_t+\gamma\cdot\Delta t\{\ddot{u}\}_{t+\Delta t}$$

4. Analysis of Annual Average Exceeding Probability of Wind Resistance Demand of Membrane Roofs

4.1. Analytical Steps

① Wind hazard analysis. Define the wind field intensity measure IM in a specific area and obtain the annual average exceeding probability $\lambda(IM)$ of IM, which is expressed by the annual average exceeding probability $\lambda(V_m)$ of the design maximum wind speed, that is, the design wind speed hazard curve.

② Structural analysis: Structural response analysis is performed to obtain the response values of the membrane roof under different wind field intensities IM, that is, the exceedance probability $G(EDP|IM)=P(EDP>d|IM)$ of the engineering demand parameter (EDP). Based on this, the annual average exceedance probability $\lambda(EDP)$ of the EDP is determined. For the membrane roof, the maximum vertical deformation of the structure is selected as the EDP.

③ Exceedance probability analysis: The limit state (DM) that meets the performance level of membrane roofs is defined. In this paper, the maximum deformation limit of membrane roofs in "Technical Specification for Membrane Structures" (CECS158:2015) [54] is

taken as the evaluation standard of wind resistance performance. On this basis, $G(DM|EDP)$ is calculated and $\lambda(DM)$ is obtained.

Based on the above analysis, the wind resistance evaluation for the membrane roof can be carried out. The derivation process in this study does not consider the random characteristics of DM, that is, $\lambda(DM) = \lambda(EDP)$. Therefore, the equation of the average annual exceedance probability of the wind resistance demand for membrane roofs is as follows:

$$\lambda(DM) = \lambda(EDP) = \int G(EDP|IM)d\lambda(IM) \tag{37}$$

4.2. Theoretical Derivation

The annual mean exceedance probability for wind resistance requirements of membrane roofs can be determined using probabilistic statistical methods (such as the Monte Carlo method and the subspace simulation method). However, these methods are based on large sample data. For more complex and large-scale membrane structures, the computational effort is considerable, and the efficiency is low. In this paper, the method of deriving the closed-form expression for the annual mean exceedance probability of structural seismic limit states by F. Jalayer [15] is referenced. Under appropriate assumptions, a simplified calculation expression for the annual mean exceedance probability of wind resistance requirements is obtained, facilitating probabilistic assessment for wind-resistant design of large-span membrane roofs. The following assumptions are made:

① The maximum design wind speed hazard curve is used to describe wind field intensity and is fitted using a quintic polynomial:

$$\lambda(x) = c_0 + c_1x + c_2x^2 + c_3x^3 + c_4x^4 + c_5x^5$$

② Considering the nonlinear vibration characteristics of a membrane roof, according to the frequency domain analysis process, the root mean square of the structural displacement response is the square root of the integral of the power spectrum over the frequency domain, which is related to the wind speed spectrum value. Previous experimental results have also shown that there is a power series relationship between the mean structural response and the wind speed spectrum value. Therefore, the structural wind-resistant displacement demand can be approximately expressed as a power function of the wind speed value, that is $\eta_{EDP} = a(V)^b$.

③ Considering the fluctuating wind speed as a zero-mean Gaussian stationary random process, it is assumed that under specific site conditions, the wind resistance demand (EDP) of the structure follows a log-normal distribution, that is $EDP - LN(\eta_{EDP}, \sigma^2_{EDP})$. Where η_{EDP} and σ_{EDP} represent the mean and standard deviation of the structural wind resistance demand (EDP). It is further assumed that σ_{EDP} remains constant for different wind speeds at the same site and does not change with variations in wind speed, as shown in Figure 4.

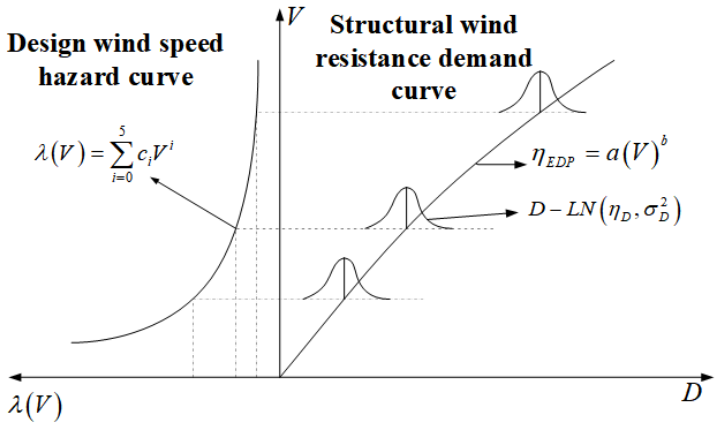

Figure 4. Design wind speed hazard curve and roof wind resistant demand curve.

According to Equation (37), the annual average exceedance probability of structural wind resistance demand $D > d$ is as follows:

$$\begin{aligned}\lambda(d) &= \int G(d|V)d\lambda(V)\\ &= \int P(D>d|V)d\lambda(V)\\ &= \int \frac{dP(D>d|V)}{dV}\lambda(V)\,dV\end{aligned} \tag{38}$$

since

$$\begin{aligned}P(D>d|V) &= 1-P(D\le d|V) = 1-P(\ln D\le \ln d|V)\\ &= 1-P\left(\frac{\ln D-\ln\tilde{D}}{\sigma_D}\le\frac{\ln d-\ln\tilde{D}}{\sigma_D}|V\right)\\ &= 1-P\left(\frac{\ln D-\ln\eta_D}{\sigma_D}\le\frac{\ln d-\ln\eta_D}{\sigma_D}|V\right)\\ &= 1-\Phi\left(\frac{\ln(d/\eta_D)}{\sigma_D}\right)\end{aligned} \tag{39}$$

where $\Phi(\cdot)$ is the standard normal distribution function.

Then,

$$\begin{aligned}\frac{dP(D>d|V)}{dV} &= \frac{d}{dV}\left\{1-\Phi\left(\frac{\ln(d/\eta_D)}{\sigma_D}\right)\right\} = -\frac{d}{dV}\left\{\Phi\left(\frac{\ln(d/\eta_D)}{\sigma_D}\right)\right\}\\ &= -\frac{d}{dV}\left\{\Phi\left(\frac{\ln d-\ln\eta_D}{\sigma_D}\right)\right\} = -\frac{d}{dV}\left\{\Phi\left(\frac{\ln d-\ln\left(a(V)^b\right)}{\sigma_D}\right)\right\}\end{aligned} \tag{40}$$

Equation (40) can be rearranged as follows:

$$\frac{dP(D>d|V)}{dV} = \frac{b}{V\sigma_D}\Phi\left(\frac{\ln d-\ln\left(a(V)^b\right)}{\sigma_D}\right) \tag{41}$$

Substituting Equation (41) into Equation (38) yields the following:

$$\begin{aligned}\lambda(d) &= \int \frac{b}{V\sigma_D}\Phi\left(\frac{\ln d - \ln\left(a(V)^b\right)}{\sigma_D}\right)\lambda(V)dV \\ &= \int \frac{b}{V\sigma_D}\frac{1}{\sqrt{2\pi}}e^{-\frac{1}{2}\left(\frac{\ln d-\ln\left(a(V)^b\right)}{\sigma_D}\right)^2}\lambda(V)dV\end{aligned} \tag{42}$$

Based on the above analysis, the following can be obtained:

$$\lambda(V) = c_0 + c_1V + c_2V^2 + c_3V^3 + c_4V^4 + c_5V^5 = \sum_{i=0}^{5} c_iV^i \tag{43}$$

$$\begin{aligned}\lambda(d) &= \int \frac{b}{V\sigma_D}\frac{1}{\sqrt{2\pi}}e^{-\frac{1}{2}\left[\frac{\ln d-\ln\left(a(V)^b\right)}{\sigma_D}\right]^2}\sum_{i=0}^{5} c_iV^i dV \\ &= \sum_{i=0}^{5}\int \frac{b}{V\sigma_D}\frac{1}{\sqrt{2\pi}}\cdot e^{-\frac{1}{2}\left[\frac{\ln d-\ln\left(a(V)^b\right)}{\sigma_D}\right]^2} c_iV^i dV \\ &= \sum_{i=0}^{5} c_i\int \frac{b}{V\sigma_D}\frac{1}{\sqrt{2\pi}}e^{-\frac{1}{2}\left[\frac{\ln d-\ln\left(a(V)^b\right)}{\sigma_D}\right]^2} e^{i\ln V}dV \\ &= \sum_{i=0}^{5} c_ie^{\left[\frac{1}{2}i^2\left(\frac{\sigma_D}{b}\right)^2\right]}e^{i\ln\left(\frac{d}{a}\right)^{\frac{1}{b}}}\cdot\int \frac{b}{V\sigma_D}\frac{1}{\sqrt{2\pi}}e^{-\frac{1}{2}\left[\frac{\ln V-\left[\ln\left(\frac{d}{a}\right)^{\frac{1}{b}}+i\left(\frac{\sigma_D}{b}\right)^2\right]}{\frac{\sigma_D}{b}}\right]^2}dV\end{aligned} \tag{44}$$

Letting $\psi = \left[\frac{\ln V-\left[\ln\left(\frac{d}{a}\right)^{\frac{1}{b}}+i\left(\frac{\sigma_D}{b}\right)^2\right]}{\frac{\sigma_D}{b}}\right]$, then $d\psi = \frac{b}{V\sigma_D}dV$. Substituting this into Equation (44) yields the following:

$$\begin{aligned}\lambda(d) &= \sum_{i=0}^{5} c_ie^{\left[\frac{1}{2}i^2\left(\frac{\sigma_D}{b}\right)^2\right]}e^{i\ln\left(\frac{d}{a}\right)^{\frac{1}{b}}}\cdot\int \frac{1}{\sqrt{2\pi}}e^{-\frac{1}{2}\psi^2}d\psi = \sum_{i=0}^{5} c_ie^{\left[\frac{1}{2}i^2\left(\frac{\sigma_D}{b}\right)^2\right]}e^{i\ln\left(\frac{d}{a}\right)^{\frac{1}{b}}}\cdot 1 \\ &= \sum_{i=0}^{5} c_i\left[\left(\frac{d}{a}\right)^{\frac{1}{b}}\right]^i e^{\left[\frac{1}{2}i^2\left(\frac{\sigma_D}{b}\right)^2\right]}\end{aligned} \tag{45}$$

The expression for the annual mean exceedance probability of the structural wind resistance demand D > d is as follows:

$$\lambda(d)=\sum_{i=0}^{5}c_i\left[\left(\frac{d}{a}\right)^{\frac{1}{b}}\right]^{i}e^{\left[\frac{1}{2}i^2\left(\frac{\sigma_D}{b}\right)^2\right]}=c_0+c_1\left(\frac{d}{a}\right)^{\frac{1}{b}}e^{\left[\frac{1}{2}\left(\frac{\sigma_D}{b}\right)^2\right]}+c_2\left[\left(\frac{d}{a}\right)^{\frac{1}{b}}\right]^{2}e^{\left[2\left(\frac{\sigma_D}{b}\right)^2\right]}$$
$$+c_3\left[\left(\frac{d}{a}\right)^{\frac{1}{b}}\right]^{3}e^{\left[\frac{9}{2}\left(\frac{\sigma_D}{b}\right)^2\right]}+c_4\left[\left(\frac{d}{a}\right)^{\frac{1}{b}}\right]^{4}e^{\left[8\left(\frac{\sigma_D}{b}\right)^2\right]}+c_5\left[\left(\frac{d}{a}\right)^{\frac{1}{b}}\right]^{5}e^{\left[\frac{25}{2}\left(\frac{\sigma_D}{b}\right)^2\right]} \quad (46)$$

where c_i is the fitting coefficient of the wind speed spectrum hazard curve, d is the maximum allowable vertical deformation of the membrane roof, a and b are the fitting curve parameters for the mean structural response η_D, and σ_D is the standard deviation of the membrane roof's response.

4.3. Example Analysis

Taking the membrane roof as an example, the membrane elastic modulus E1 = 1400 MPa, E2 = 900 MPa, = 1.226 kg/m^3, and the membrane thickness h = 0.001 m. The length and width of the roof structure are A and B, respectively. The initial pre-tension was 3 kN. The natural frequency of the roof structure is 0.28 Hz. Due to the significant flexibility exhibited by the membrane roof, Section 5.3.4 of the "Technical Specification for Membrane Structures" (CECS158:2015) stipulates [54]:

When designing for the normal serviceability limit state, the deformation of the membrane structure must not exceed the specified limit values. For fully tensioned and cable-supported membrane structures, the maximum displacement under the first load effect combination should not exceed 1/250 of the span or 1/125 of the cantilever length; under the second load effect combination, it should not exceed 1/200 of the span or 1/100 of the cantilever length. As the membrane roof is a fully tensioned type, considering wind loading as the second load effect combination, the maximum deformation U_m of the membrane surface is taken as the engineering demand parameter (EDP) when performing the wind resistance probability assessment for the membrane roof.

① Wind hazard analysis

In the wind hazard analysis, the average annual exceedance probability of the maximum design wind speed is used in this paper. The average annual exceedance probability curve for the design wind speed in the Hangzhou area is shown in Figure 3. A polynomial fitting is applied to simplify the curve, and the coefficients of the fitted polynomial are calculated as follows:

$$c_0=1.52,\ c_1=-0.4042,\ \ c_2=0.0486,\ c_3=-0.003117$$

$$c_4=0.0001027,\ c_5=-1.357\times10^{-6}$$

② Structural Analysis

To calculate the membrane structure response under different wind intensities, the Newmark-β method is used in this paper for time-domain analysis of the membrane roof. Three calculation conditions corresponding to design return periods of 10 years, 50 years, and 100 years in the Hangzhou area are considered for the analysis. The wind direction is along the *x*-axis, with a wind angle of 0°. The wind pressure time histories at each point are converted into wind load time histories, and the Newmark-β method is applied for wind-induced vibration time history analysis of the membrane roof. The peak displacement responses of the membrane surface under the design return periods of 10 years, 50 years, and 100 years are obtained. The analysis results are shown in Table 3.

Table 3. Peak response of membrane roof.

Working Condition	10 Years	50 Years	100 Years
1	0.1449	0.2311	0.2806
2	0.1668	0.2343	0.3082
3	0.1580	0.2539	0.2618
4	0.1500	0.2515	0.2925
5	0.1586	0.2172	0.3189
6	0.1730	0.2461	0.2926
7	0.1535	0.2231	0.2038
8	0.1625	0.2710	0.2746
9	0.1469	0.2429	0.2891
10	0.1539	0.2517	0.3120
Mean	0.1574	0.2342	0.2705
Standard deviation	0.0082	0.0135	0.0314

The statistical data from the table can be used to obtain a fitted curve for the peak displacement response mean value of the membrane roof. The parameters of the fitted curve are shown in the table below:

The statistical data from the table can be used to obtain a fitted curve for the peak displacement response mean value of the membrane roof $\eta_{EDP} = a(V)^b$, The parameters of the fitted curve are shown in Table 4.

Table 4. Mean fitting curve parameters for displacement peak response of membrane roofs.

Basic Wind Pressure	Wind Speed Value	Maximum Response Mean Value	a	b
0.25	20.00	0.1574		
0.4	25.30	0.2342	6.476×10^{-4}	1.83
0.45	26.83	0.2705		

Substituting the parameters into Equation (46), the closed-form expression for the annual mean exceedance probability of the peak displacement response of the membrane roof can be obtained as follows:

$$\lambda(d) = 1.52 - 0.4042\left(\frac{d}{0.024}\right)^{\frac{1}{0.67}} e^{\left[\frac{1}{2}\left(\frac{0.0385}{0.67}\right)^2\right]} + 0.0486\left[\left(\frac{d}{0.024}\right)^{\frac{1}{0.67}}\right]^2 e^{\left[2\left(\frac{0.0385}{0.67}\right)^2\right]}$$

$$-0.003117\left[\left(\frac{d}{0.024}\right)^{\frac{1}{0.67}}\right]^3 e^{\left[\frac{9}{2}\left(\frac{0.0385}{0.67}\right)^2\right]} + 0.0001027\left[\left(\frac{d}{0.024}\right)^{\frac{1}{0.67}}\right]^4 e^{\left[8\left(\frac{0.0385}{0.67}\right)^2\right]}$$

$$-1.357\times10^{-6}\times\left[\left(\frac{d}{0.024}\right)^{\frac{1}{0.67}}\right]^5 e^{\left[\frac{25}{2}\left(\frac{0.0385}{0.67}\right)^2\right]}$$

Through these calculations, the annual mean exceedance probabilities corresponding to different membrane roof displacement requirements can be obtained. The results are shown in Table 5.

Table 5. Probabilistic evaluation of displacement requirements for the membrane roof.

Displacement Demand	L/300	L/250	L/200	L/150	L/125
Annual Mean Exceedance Probability	51.68%	29.19%	16.12%	6.78%	3.20%
Response Return Period (years)	1.93	3.43	6.20	14.75	31.25

Note: *L* is taken as the length of the long side of the membrane roof.

The annual average exceedance probability curve of the peak displacement response of the membrane roof (the displacement demand hazard curve) is shown in Figure 5.

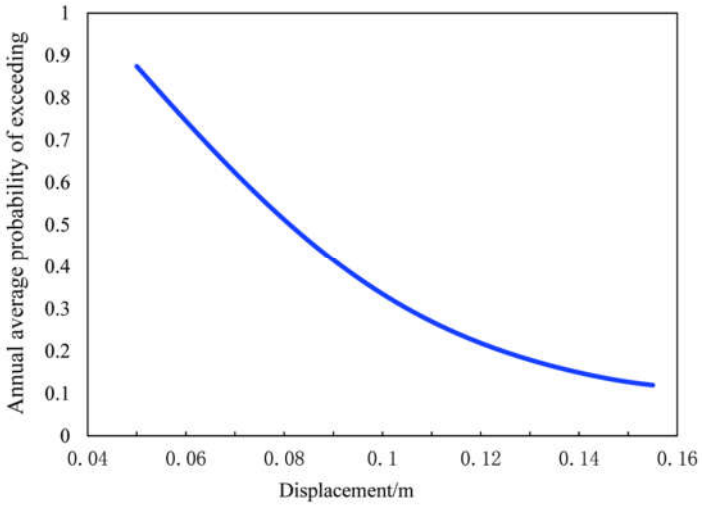

Figure 5. Displacement demand hazard curve.

Using the closed-form expressions derived in this paper, the annual average exceedance probability and the maximum response recurrence period for the membrane roof under different deformation requirements can be obtained with minimal computation. The method proposed in this paper provides a theoretical foundation for solving the exceedance probability for different internal force requirements, acceleration requirements, and other indicators for subsequent membrane roof structures. This allows for a probabilistic performance evaluation of the wind resistance design of membrane roofs.

5. Probabilistic Wind Resistance Evaluation Process for Membrane Roofs Based on Aerodynamic Stability

5.1. Current Wind Resistance Design Process for Membrane Structures

The traditional wind resistance design process for membrane structures is shown in Figure 6a.

(1) Basic information such as initial shape, geometric material parameters, and pre-tension of the structure is given in advance.

(2) The wind load information obtained from the pressure test of the rigid model is loaded on the finite element nodes of the structure, and the wind-induced vibration response analysis is carried out to obtain the response information concerned by the wind resistance design of the structure. When the structural response is greater than or equal to the design limit, the pre-tension or geometric material parameters of the structure need to be adjusted, and the wind-induced vibration response analysis should be carried out again. When the extreme response is less than the design limit, it is considered that the membrane structure meets the design requirements.

The wind-resistant design method of tensile membrane structure to prevent aeroelastic instability was first proposed by Dr. Chen Zhaoqing of Harbin Institute of Technology in 2015 [55]. The flow chart is shown in Figure 6b:

Basic information such as the initial shape, geometric material parameters, and pretension of the structure is given in advance.

Determine the critical wind speed Vcr of aeroelastic instability of the structure. If the critical wind speed Vcr is less than or equal to the local design wind speed Vd, adjustments to the structure's initial shape, geometric dimensions, and prestress are necessary, followed by revalidation until the critical wind speed Vcr exceeds the design wind speed.

Determine the additional aerodynamic forces on the membrane structure, including the additional air mass and aerodynamic damping.

Using the simplified aeroelastic model test method, the fluid-structure coupling between membrane structure and air is considered by adjusting the mass and damping matrix of the structure. Wind load data obtained from pressure measurements on a rigid model in wind tunnel tests are then applied to the finite element nodes of the structure for wind vibration response analysis. If the extreme response is greater than or equal to the design requirements, adjustments to the structure's prestress or material parameters are made, and the wind vibration response analysis is rerun until the response is within the design limits.

After Dr. Zhao-Qing Chen proposed the wind resistance design method for tensile membrane structures to prevent aeroelastic instability, subsequent studies on membrane structure wind resistance design have largely focused on optimizing the wind vibration response analysis process or studying wind pressure distribution patterns. Due to the randomness of wind fields, this randomness manifests in the fact that the interference curves measured at the same basic wind speed vary over time. Therefore, based on the optimization of wind resistance design to prevent aeroelastic instability, this paper proposes a probabilistic evaluation method for wind resistance design of membrane roofs that takes aerodynamic stability into account. This approach aims to provide a probabilistic perspective for evaluating and assisting with design.

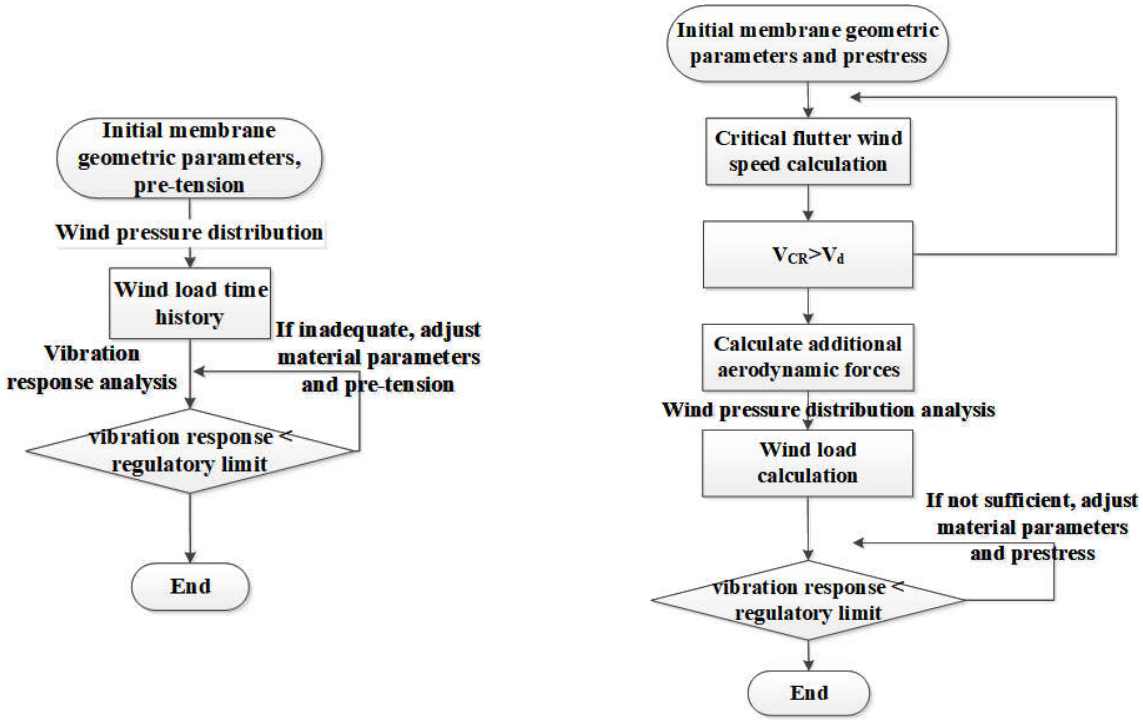

(**a**) (**b**)

Figure 6. Wind resistant design flow chart of membrane structure. (**a**) The traditional wind-resistant design process; (**b**) The anti-wind design process to prevent gas projectile instability.

5.2. Probabilistic Wind Resistance Evaluation Process for Membrane Roofs Considering Aerodynamic Stability

Research has shown that reasonable design principles for preventing aeroelastic instability in membrane roofs include the relationship between the membrane material's warp and weft directions and the wind direction, proper control of prestress, and the control of the span ratio in the crosswind direction [56–59]. Due to the constraints imposed by the overall structural plan, the span ratio in the crosswind direction is generally a deterministic parameter, with the only variable being the determination of prestress. Therefore, in the probabilistic evaluation method for wind resistance design of membrane roofs considering aerodynamic stability, the first step is to determine the minimum prestress level required to prevent membrane aeroelastic instability, based on the pre-given reasonable layout of the structural geometric and material parameters. The flowchart for the Probabilistic wind resistance evaluation method for membrane roofs considering aerodynamic stability is depicted in Figure 7.

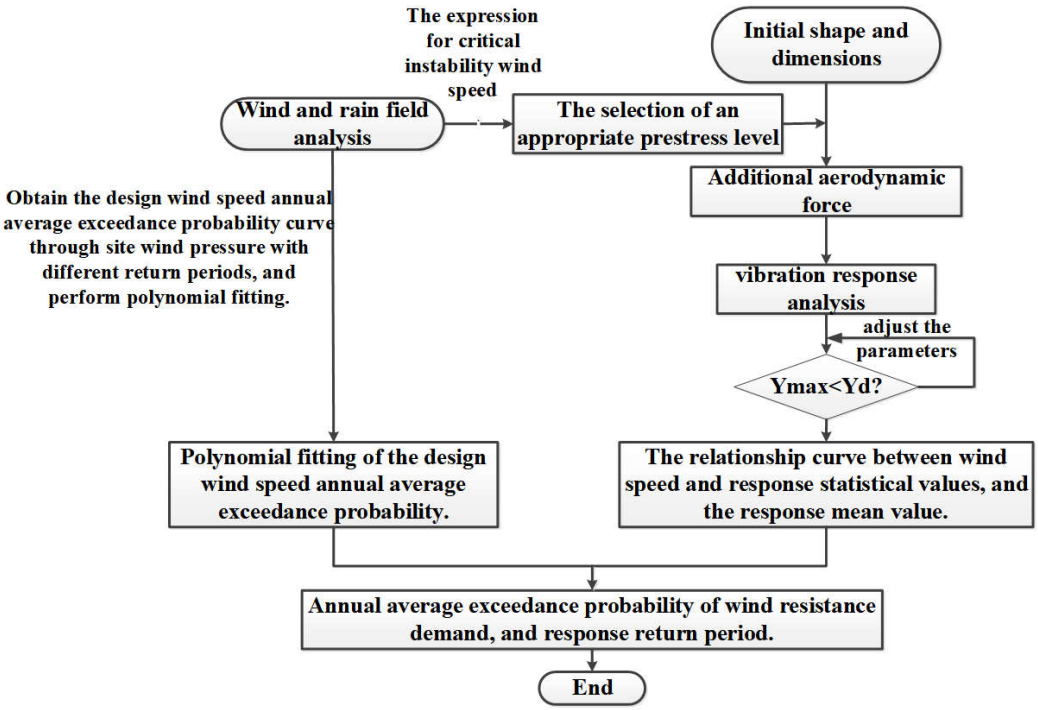

Figure 7. Wind resistance reliability of membrane roof considering aerodynamic stability.

The specific process is as follows:

① The reasonable initial shape, geometric size, and basic wind pressure of the membrane roof are given in advance.

② Through the expression for critical instability wind speed, the design's critical instability wind speed must be less than or equal to the local maximum design wind speed. Therefore, based on this analytical expression, the minimum range of prestress can be determined, and a reasonable prestress level is selected.

③ Back-calculate the design maximum wind speed using the basic wind pressure within the site recurrence period, obtain the corresponding annual average exceedance probability curve for the design maximum wind speed, and fit it using a polynomial.

④ According to the additional air quality calculation formula, substitute the corresponding geometric material parameters and the corresponding design wind speed to obtain the additional air quality corresponding to the recurrence period.

⑤ For different local design recurrence periods, take at least 10 simulated data samples of the fluctuating wind speed for each recurrence period scenario and perform a nonlinear time history analysis of the roof. During the time history analysis, consider the impact of the added mass to account for the coupling effect between the membrane roof and the fluid. Load the wind load information obtained from rigid model pressure tests or numerical wind tunnel simulations onto the structural finite element nodes and obtain the displacement response of the membrane roof.

⑥ Statistically analyze the peak response of the membrane roof to obtain the mean value and standard deviation. Furthermore, derive the fitting curve for the hazard of the design wind speed and the fitting curve coefficients for the corresponding average peak displacement response of the membrane roof.

⑦ Using the displacement demand fff as the performance level point, determine the annual average exceedance probability of the wind resistance demand and the response recurrence period.

5.3. Determination of Reasonable Prestress for Membrane Roofs

The critical wind speed expressions of aeroelastic instability of closed membrane roofs and open membrane roofs are given in reference [49].

Closed membrane roofs are calculated as follows:

$$V_{cr} = \sqrt{\frac{4\pi\left(m^2\pi^2b^2N_{0x} + n^2\pi^2a^2N_{0y}\right) + 3\varepsilon f^2\left(\rho\pi a^2b^2 + 4\rho_0 ab\alpha_1\right)}{8\pi b\rho_0 m\alpha_3}} \tag{47}$$

Open membrane roofs are calculated as follows:

$$V_{cr} = \pi\sqrt{\frac{m^2bN_{0x}/4a + n^2aN_{0y}/4b + 3hm^2n^2\pi^2(\alpha+\beta)f^2/8ab}{\rho_0 a\frac{ab}{MN}\sum_{j=1}^{M\times N} a_{1j}\sin\frac{m\pi x_j}{a}\sin\frac{n\pi y_j}{b}}} \tag{48}$$

The research approach for the reasonable arrangement of parameters for membrane roofs in a specific site involves ensuring that, after rational arrangement, the roof does not experience divergent instability within the design recurrence period. Therefore, the initial prestress and geometric parameters of the membrane roof should meet the following condition: the local design maximum wind speed must be less than or equal to the critical instability wind speed.

$$V \le V_{cr} \tag{49}$$

According to the above principle, determine the parameters for the minimum prestress and span ratio of the membrane roof.

Substituting Equation (46) into Equation (48) yields the following:

$$V \le \sqrt{\frac{4\pi\left(m^2\pi^2b^2N_{0x} + n^2\pi^2a^2N_{0y}\right) + 3\varepsilon f^2\left(\rho\pi a^2b^2 + 4\rho_0 ab\alpha_1\right)}{8\pi b\rho_0 m\alpha_3}} \tag{50}$$

where V is the local design wind speed. For Equation (49), the prerequisite for the inequality to always hold is that the minimum value of the term on the right side must be greater than the design wind speed, calculated as follows:

$$V \le \left(\sqrt{\frac{4\pi\left(m^2\pi^2b^2N_{0x}+n^2\pi^2a^2N_{0y}\right)+3\varepsilon f^2\left(\rho\pi a^2b^2+4\rho_0 ab\alpha_1\right)}{8\pi b\rho_0 m\alpha_3}} \right)_{\min} \tag{51}$$

Rearranging and simplifying the above equation yields the following:

$$N_{0x}+\frac{a^2}{b^2}N_{0y} \ge \frac{2\rho_0\alpha_3}{b\pi}V^2 \tag{52}$$

Equation (52) represents the minimum prestress standard for ensuring aerodynamic stability in closed membrane roofs. Once the span ratio in the crosswind direction is determined, the minimum prestress value can be obtained. Similarly, the condition for the minimum prestress value that ensures aerodynamic stability in open membrane roofs is calculated as follows:

$$N_{0x}+\frac{a^2}{b^2}N_{0y} \ge \frac{4a^3\rho_0}{\pi}V^2\cdot\frac{1}{MN}\sum_{j=1}^{M\times N}a_{1j}\sin\frac{m\pi x_j}{a}\sin\frac{n\pi y_j}{b} \tag{53}$$

The values of a and b are determined based on the structural layout, and by substituting them into Equations (52) and (53), the minimum prestress value can be obtained.

6. Conclusions

In this paper, a probabilistic assessment method for wind-resistant design of membrane roofs, considering aerodynamic stability for a specific wind field probability model, is established through theoretical analysis. The wind resistance performance of the membrane roof is evaluated using the average annual exceedance probability. The closed-form expression for the annual average exceedance probability of the wind resistance demand for membrane roofs has been obtained. Based on this, the wind resistance probability evaluation method for membrane roofs considering aerodynamic stability has been proposed, along with specific steps and relevant analytical formulas for this method. The specific conclusions are as follows:

(1) In the analysis, we employed the Type I extreme value distribution to characterize the site wind, assuming that the turbulent wind speed can be modeled as a zero-mean stationary stochastic process. This approach enables us to simplify the derivation of the closed-form expression for the annual average exceedance probability of the wind resistance demands for membrane roofs by fitting the annual average exceedance probability curve corresponding to the design wind speed with a fifth-order polynomial.

(2) The methodology in our paper enables the calculation of exceedance probabilities for various deformation demands of the membrane roof. Additionally, it can be applied to assess the exceedance probabilities for different internal force and acceleration requirements, among other response requirements. This significantly reduces the computational effort required for the analysis.

(3) Building on these findings, we have formulated a wind resistance probability evaluation method for membrane roofs that incorporates aerodynamic stability. We have detailed the specific steps and relevant analytical formulas for this method, thereby enriching the theoretical framework for wind-resistant design of membrane roofs. This contribution addresses a gap in the theoretical research on probabilistic assessment for the wind-resistant design of tensile membrane structures.

(4) Based on these findings, we have formulated a wind resistance probability assessment method for membrane roofs that incorporates aerodynamic stability. We have provided a detailed explanation of the specific steps and relevant analytical formulas associated with this method, thereby enriching the theoretical framework for the

wind-resistant design of membrane roofs. This contribution fills a gap in the theoretical research on probabilistic assessment for the wind-resistant design of tensile membrane structures.

(5) The proposed method further ensures the structural safety of tensile membrane roofs under wind loads. It provides a comprehensive approach to evaluating the wind resistance of membrane roofs, taking into account the complex interactions between wind forces and the roof's aerodynamic properties. This advancement in the field is crucial for the development of more reliable and safe membrane roof designs that can withstand the challenges posed by wind loads under various environmental conditions.

Author Contributions: Conceptualization, W.S.; methodology, H.L.; software, W.S.; validation, W.S., H.L. and H.Y.; formal analysis, H.Y.; investigation, H.Y.; resources, H.Y.; data curation, W.S.; writing—original draft preparation, W.S.; writing—review and editing, H.L.; visualization, W.S.; supervision, H.Y.; project administration, W.S.; funding acquisition, W.S. All authors have read and agreed to the published version of the manuscript.

Funding: This research received no external funding.

Data Availability Statement: The original contributions presented in this study are included in the article. Further inquiries can be directed to the corresponding author.

Conflicts of Interest: Authors Weiju Song and Heding Yu were employed by Huasheng Construction Group Co., Ltd. The remaining author declares that the research was conducted in the absence of any commercial or financial relationships that could be construed as a potential conflict of interest.

References

1. Lai, G.; He, Y.; Zhao, Y.Z.L. Influence of Friction Coefficient between Cable and Membrane on Wind-Induced Response of Air-Supported Membrane Structures with Oblique Cable Net. *Buildings* **2023**, *13*, 649. https://doi.org/10.3390/buildings13030649.
2. Zhang, Q. Membrane structure technology research and application progress. *Constr. Technol.* **2010**, *39*, 1–5.
3. Zhang, Z.; Liu, C.; Zheng, Z.; Liu, J.; Zhang, M. Nonlinear dynamic response of umbrella-shaped membrane structures under hail load. *J. Civ. Environ. Eng. (Chin. Engl.)* **2023**, *45*, 79–89.
4. Lu, D.; Lou, W.; Yang, Y. Study on aerodynamic damping effect of wind-induced fluid-structure coupling in cable membrane structures. *Vib. Shock.* **2013**, *32*, 47–53.
5. Wu, F.; Ji, X.; Huang, G.; Ji, X.; Zhao, Y.-G. Wind-induced vulnerability analysis of low-rise building envelopes based on simplified progressive failure. *J. Build. Struct.* **2021**, *42*, 32–39.
6. Tomokiyo, E.; Nishijima, K. Characteristics and damage of houses suffered from strong wind due to typhoon Faxai (2019). *J. Technol. Des.* **2022**, *28*, 1089–1094.
7. Wang, Z.; Wang Y.; Yu, B.; Xu, Q.; He, Y.; Li, Z. Experimental study on the wind pressure characteristics of a UHV converter station roof in different wind fields. *J. Vib. Shock.* **2024**, *43*, 146-155.
8. Zhao, Y.; Feng, L.; Chen, H. Study on wind resistance uplift test and reinforcement measures of fan-shaped curved metal roofs. *Build. Technol.* **2024**, *55*, 1343–1346.
9. Zhang, H.; Wang, T.; Li, Z.; Lu, D.G. Wind disaster vulnerability assessment of airport terminal roof truss systems based on wind tunnel tests and multiple performance levels. *J. Build. Struct.* **2024**, *45*, 189–199.
10. Salahuddin, H.; Qureshi, L.A.; Nawaz, A.; Abid, M.; Alyousef, R.; Alabduljabbar, H.; Aslam, F.; Khan, S.F.; Tufail, R.F. Elevated Temperature Performance of Reactive Powder Concrete Containing Recycled Fine Aggregates. *Materials* **2020**, *13*, 3748.
11. Farhan Mushtaq, S.; Ali, A.; Khushnood, R.A.; Tufail, R.F.; Majdi, A.; Nawaz, A.; Durdyev, S.; Burduhos Nergis, D.D.; Ahmad, J. Effect of Bentonite as Partial Replacement of Cement on Residual Properties of Concrete Exposed to Elevated Temperatures. *Sustainability* **2022**, *14*, 11580.
12. Zou, Y.; Lu, X. Seismic design theory and methods based on structural performance. *Ind. Archit.* **2006**, *36*, 1–7.
13. Collins, K.R.; Wen, Y.K.; Foutch, D.A. Dual-level design: A reliability-based methodology. *Earthq. Eng. Struct. Dyn.* **1996**, *25*, 1433–1467.
14. Deierlein, G.G.; Krawinkler, H.; Cornell, C.A. A framework for performance-based earthquake engineering. In Proceedings of the Pacific Conference on Earthquake Engineering, Christchurch, New Zealand, 13–15 February 2003.
15. Jalayer, F. Direct Probabilistic Seismic Analysis: Implementing Non-Linear Dynamic Assessments. Ph.D. Thesis, Stanford University, Stanford, CA, USA, 2003.
16. Luo, N.; Zhao, G. Wind resistance dynamic reliability of high-rise and tall structures. *J. Dalian Univ. Technol.* **2002**, *42*, 208–212.
17. Zhang, L. Research on Stochastic Wind Fields and Wind Resistance Reliability Analysis of Tall and High-Rise Structures. Ph.D. Thesis, Tongji University, Shanghai, China, 2006.

18. Liu, X. Wind Vibration Reliability Research of High-Rise Buildings Based on Comfort Criteria. Master's Thesis, Chongqing University, Chongqing, China, 2013.
19. Feng, Y. Research on Wind-Induced Vibration Comfort Evaluation Standards for High-Rise Buildings Based on Reliability. Master's Thesis, Harbin Institute of Technology, Harbin, China, 2017.
20. Yang, C.; Wu, Y.; Shi, S.; Mo, Z. Reliability study of wind vibration comfort of wind-sensitive high-rise structures. *J. Guangzhou Univ. (Nat. Sci. Ed.)* **2018**, *17*, 58–65.
21. Tan, C.; Zhang, W.; Liu, Z. Wind resistance reliability analysis of transmission tower-line systems based on probability density evolution. *J. Comput. Mech.* **2024**, *41*, 409–414.
22. Paulotto, C.; Augusti, G.; Ciampoli, M. Some proposals for a first step towards a performance based wind engineering. In Proceedings of the IFED—International Forum in Engineering Decision Making, Stoos, Switzerland, 5–9 December 2004.
23. Augusti, G.; Ciampoli, M. First steps towards performance-based wind engineering. In *Performance of Wind Exposed Structures: Results of the PERBACCO Project*; Firenze University Press: Firenze, Italy, 2006; p. 13.
24. Augusti, G.; Ciampoli, M. Performance-based design in risk assessment and reduction. *Probabilistic Eng. Mech.* **2008**, *23*, 496.
25. Petrini, F.; Bonternpi, F.; Ciampoli, M. Performance-based wind engineering as a tool for the design of the hangers in a suspension bridge. In Proceedings of the 4th International ASRANet Colloquium, Athens, Greece, 25–27 June 2008.
26. John, W.; Thang, N. Performance-based wind engineering for wood-frame buildings. *J. Struct. Eng.* **2009**, *135*, 169.
27. Petrini, F.; Ciampoli, M.; Augusti, G. A probabilistic framework for performance-based wind engineering. In Proceedings of the Fifth European and African Conference on Wind Engineering, Florence, Italy, 19–23 July 2009.
28. Zhou, Y.; Wang, D.; Chen, X. Performance-based structural wind resistance design theory framework. *J. Disaster Prev. Mitig. Eng.* **2009**, *29*, 244–251.
29. He, M.; Li, X. Performance-based wind resistance design of tall structures. *Vib. Shock.* **2013**, *32*, 87–94, 105.
30. Liu, X.; Huang, G.; He, H.; Zheng, H. Probabilistic assessment of wind-induced damage to roof coverings. *Natl. Struct. Eng. Acad. Conf.* **2014**, 349–354.
31. Huang, G.; Luo, Y.; Zheng, H.; Liu, X.; He, H. Wind-induced roof covering damage assessment considering wind speed variability. *J. Civ. Eng.* **2016**, 64–71.
32. Ji, X.; Huang, G.; Luo, Y.; Zhang, J. Wind-induced vulnerability analysis of roof systems based on Copula function considering wind load correlation. *J. Build. Struct.* **2018**, *39*, 138–145.
33. Li, Z.; Hu, J.; Wang, T. Wind disaster vulnerability analysis of standing seam roof systems based on fuzzy performance levels. *Eng. Mech.* **2024**, *41*, 180–190.
34. Zhang, H.; Yin, H.; Liu, P.; Zhang, X.; Dong, C. Impact of window and door system failure on wind-induced vulnerability of light steel roof structures. *J. Shenyang Jianzhu Univ. (Nat. Sci. Ed.)* **2023**, *39*, 71–78.
35. Wu, F.; Yao, X.; Zhou, H.; Huang, G.; Nie, S.; Ji, X.; Gong, T. Wind-induced vulnerability analysis of light steel houses as a whole. *Vib. Shock.* **2024**, *43*, 84–93.
36. Der Kiureghian, A.; Ditlevsen, O. Aleatory or epistemic? Does it matter? *Struct. Saf.* **2009**, *31*, 105–112.
37. Gu, M.; Lu, H. Research progress on wind load and wind-induced response of membrane structures. *Vib. Shock.* **2006**, *25*, 25.
38. Pang, W.; Bai, G.; Teng, Y.; Wang, L. Application of P-III and Extreme Value I distribution curves in maximum wind speed calculation. *Meteorol. Sci. Technol.* **2009**, *37*, 221–223.
39. *GB15112-10384*; Unified Standard for Reliability Design of Building Structures. China Architecture & Building Press: Beijing, China, 2002.
40. *GB50009-2012*; Code for Load Design of Building Structures. China Architecture & Building Press: Beijing, China, 2012.
41. Fu, Y.Y.; Tian, Z.K.; Li, Y.M. Regression Interpretation and Hypothesis Testing of Variance Analysis. *Stat. Decis.* **2019**, *35*, 77–80. https://doi.org/10.13546/j.cnki.tjyjc.2019.08.018.
42. Cai, D.; Li, A.; Chen, W. Analytical study on the power spectral density function of wind-induced fluctuating wind speed in the downwind direction. *Jiangsu Archit.* **1994**, 20–25.
43. Wu, H.; Xu, Y.; Hu, L.; Qing, F.; Li, Z. Fractal simulation study of near-ground fluctuating wind speed time series. *Earthq. Eng. Eng. Vib.* **2015**, *35*, 121–129.
44. Guan, Q. Extreme Wind Speed Distribution in Chongqing and Analysis of Downwind Effect of High-Rise Buildings Under Different Wind Speed Spectra. Master's Thesis, Chongqing University, Chongqing, China, 2006.
45. Li, X.; Xie, Z. Fast algorithm and application for wind vibration response and equivalent static wind load of large-span roof structures. *J. Civ. Eng.* **2010**, *43*, 29.
46. Luo, J.; Song, X. Wind vibration response of large-span membrane roofs considering the non-Gaussian characteristics of random wind pressure fields. *Civ. Archit. Environ. Eng.* **2013**, *35*, 118–123.
47. Zhang, W.F.; Ma, C.H.; Xiao, Y. Some Issues on AR Models for Wind Field Simulation. *Chin. J. Comput. Mech.* **2009**, *26*, 124–130.
48. Zhang, X.; Zhang, B.; Xin, G.H.G. Fluctuating characteristics of streamwise wind speed and total saltation mass flux in the near-neutral atmospheric surface layer. *Phys. Fluids* **2023**, *35*, 026606.
49. Ma, J.; Zhou, D.; Li, L.; Zhao, Y.-J. The Composite Approach for Wind Time Series Simulation. *Eng. Mech.* **2009**, *26*, 53–059.
50. Cheng, H.; Zhong, H. Numerical simulation of fluctuating wind speed time series. *J. Weapon Equip. Eng.* **2016**, *37*, 143–148.
51. Sun, X.; Wu, Y.; Shen, S. Numerical simulation of wind pressure distribution on flat roofs. *J. Comput. Mech.* **2007**, *24*, 294.
52. Sabetta, F.P. Estimation of response spectra and simulation of nonstationary ground motions. *Bull. Seismol. Soc. Am.* **1996**, *86*, 337–352.

53. Sun, X.; Wu, Y.; Shen, S. Study on added mass and aerodynamic damping of membrane structures. In Proceedings of the 12th National Structural Wind Engineering Conference, Xi'an, China, 19–22 October 2005; pp. 46–51.
54. *CECS158:2015*; Technical Specification for Membrane Structures. China Planning Press: Beijing, China, 2015.
55. Chen, Z. Study on the Aerodynamic Instability Mechanism of Tensile Membrane Structures. Ph.D. Thesis, Harbin Institute of Technology, Harbin, China, 2015.
56. Song, W.; Xu, J.; Wang, X.; Liu, C. Effect of Geometric Nonlinearity on Membrane Roofs Stability in Air Flow. *Shock. Vib.* **2020**, *2020*, 1–13. https://doi.org/10.1155/2020/2305145.
57. Xu, Y.-P.; Zheng, Z.-L.; Liu, C.-J.; Song, W.-J.; Long, J. Aerodynamic stability analysis of geometrically nonlinear orthotropic membrane structure with hyperbolic paraboloid. *J. Eng. Mech.* **2011**, *137*, 759–768.
58. Xu, Y.P.; Zheng, Z.L.; Liu, C.J.; Wu, K.; Song, W.J. Aerodynamic stability analysis of geometrically nonlinear orthotropic membrane structure with hyperbolic paraboloid in sag direction. *Wind. Struct.* **2018**, *26*, 355–367.
59. Liu, C.J.; Deng, X.W.; Zheng, Z.L. Nonlinear wind-induced aerodynamic stability of orthotropic saddle membrane structures. *J. Wind. Eng. Ind. Aerodyn.* **2017**, *164*, 119–127.